Dyes and Pigments 103 (2014) 34–38

Contents lists available at ScienceDirect

Dyes and Pigments

journal homepage: www.elsevier.com/locate/dyepig

High quantum efficiency and color stability in white phosphorescent organic light emitting diodes using a pyridine modified carbazole derivative

Chil Won Lee, Jun Yeob Lee*

Department of Polymer Science and Engineering, Dankook University, Jukjeon-dong, Suji-gu, Yongin-si, Gyeonggi-do 448-701, Republic of Korea

ARTICLE INFO

Article history:
Received 12 September 2013
Received in revised form
18 November 2013
Accepted 19 November 2013
Available online 28 November 2013

Keywords:
Carbazole
High triplet energy
Blue device
White device
Quantum efficiency
Color stability

ABSTRACT

A high triplet energy material derived from carbazole and pyridine, 9,9′-(5-(2-methylpyridin-3-yl)-1,3-phenylene)bis(9*H*-carbazole), was synthesized as the host material for blue and white phosphorescent organic light-emitting diodes. The 9,9′-(5-(2-methylpyridin-3-yl)-1,3-phenylene)bis(9*H*-carbazole) host showed a high triplet energy of 2.99 eV for efficient energy transfer to blue triplet emitter. High quantum efficiencies of 19.8% and 17.1% were achieved in blue and white phosphorescent organic light-emitting diodes using the 9,9′-(5-(2-methylpyridin-3-yl)-1,3-phenylene)bis(9*H*-carbazole) host material. In addition, the 9,9′-(5-(2-methylpyridin-3-yl)-1,3-phenylene)bis(9*H*-carbazole) based white phosphorescent organic light-emitting diodes showed good color stability.

1. Introduction

Phosphorescent white organic light emitting diodes (PHWOLEDs) are promising as a next generation lighting device due to high quantum efficiency and broad emission spectrum for high color rendering index. In particular, the high quantum efficiency of the PHWOLEDs is an attractive feature for a lighting device because power consumption can be reduced.

In general, the PHWOLEDs are constructed by combining a blue triplet emitter with a yellow triplet emitter, or red, green and blue triplet emitters [1–10]. The energy of the blue triplet emitter is transferred to low energy triplet emitters during the light emission process and the device performance of the PHWOLEDs are mostly dominated by the device performance of the blue phosphorescent organic light-emitting diodes (PHOLEDs). Therefore, the development of high efficiency blue PHOLEDs is important to improve the device performances of PHWOLEDs. There are several ways to improve the device performances of PHWOLEDs and one of the most efficient methods is to develop high triplet energy host materials [11–15]. Several high triplet energy host materials were reported as the host materials for the PHWOLEDs to enhance the quantum efficiency. Although high quantum efficiency was reported using various host materials, it was difficult to obtain both high quantum efficiency and color stability in the PHWOLEDs.

In this work, a high triplet energy host material derived from pyridine and carbazole, 9,9′-(5-(2-methylpyridin-3-yl)-1,3-phenylene)bis(9*H*-carbazole) (PPBC), was developed to improve the quantum efficiency and color stability of PHWOLEDs. High quantum efficiencies of 17.1% and good color stability with 0.01 change of color coordinate between 100 cd/m^2 and 10,000 cd/m^2 were demonstrated in PHWOLEDs using the PPBC host material in addition to high quantum efficiency of 19.8% in blue PHOLEDs.

2. Experimental section

Reagents and solvents were purchased at reagent grade from TCI, Aldrich, and P&H tech and used as received. All reactions were performed under a positive pressure of high purity nitrogen. The ^{1}H and ^{13}C nuclear magnetic resonance (NMR) were obtained on Avance 500 (Bruker). The FT-IR spectra for all the samples were measured using a Nicolet 380 FTIR spectrometer. High resolution mass spectra were measured on JEOL, JMS-600W spectrometer in fast atom bombardment(FAB) mode. Elemental analyses of carbon, hydrogen, and nitrogen were performed on Flash2000 (Thermofisher). Differential

---

* Corresponding author. Tel./fax: +82 31 8005 3585.
E-mail address: leej17@dankook.ac.kr (J.Y. Lee).

0143-7208/$ – see front matter © 2013 Elsevier Ltd. All rights reserved.
http://dx.doi.org/10.1016/j.dyepig.2013.11.020

scanning calorimetry (DSC) was performed on a Mettler DSC822e at a heating rate of 10 °C/min from 20 to 350 °C under argon. The photoluminescence (PL) spectra were recorded on a fluorescence spectrophotometer (HITACHI, F-7000) and the ultraviolet–visible (UV–Vis) spectra were obtained using a UV–Vis spectrophotometer (Shimadzu, UV-2501PC). Low temperature PL measurement for triplet energy analysis recorded on a PerkinElmer LS-55 in liquid nitrogen. Cyclic voltammetry (CV) was carried out in acetonitrile solution (oxidation scan) at room temperature with tetrabutylammonium perchlorate (0.1 M) was used as the supporting electrolyte. The conventional three-electrode configuration consists of a platinum working electrode, a platinum wire auxiliary electrode, and an Ag wire pseudoreference electrode with ferrocenium–ferrocene (Fc^+/Fc) as the internal standard. The synthetic route of PPBC is shown in Scheme 1.

2.1. Synthesis of 2-(3,5-dichlorophenyl)-3-methylpyridine

3-Bromo-2-methylpyridine (1.9 g, 11.04 mmol) and 3,5-dichlorophenyl boronic acid (3.16 g, 16.57 mmol) dissolved in degassed THF (60 mL) were placed into a 250 mL two necked round bottom flask. A solution of potassium carbonate (3.05 g, 22.09 mmol) in water (20 mL) was added slowly to the solution, and bubbled with nitrogen for 30 min. Finally, tetrakis(triphenylphosphine)palladium(0) (1.26 g, 1.17 mmol) was added to the above reaction mixture, then heated under reflux under nitrogen overnight. The solution was cooled to room temperature and the organics were extracted using ethyl acetate and washed with distilled water. The solution was dried over magnesium sulfate and evaporated to remove solvent. The product was further purified by flash chromatography on silica gel using methylene chloride/*n*-hexane as an eluent to produce 2.0 g (76% yield) of 2-(3,5-dichlorophenyl)-3-methylpyridine.

Yellow powder, m.p. 87 °C, FT-IR (KBr) 3051, 1557, 1423, 1407, 1383, 1293, 1254, 1190, 1097, 1034, 884, 853, 793, 765, 736, 695 cm^{-1}. ^1H NMR (500 MHz, $CDCl_3$): δ 2.50 (s, 3H), 7.19 (t, 1H, $J = 2.5$ Hz), 7.21 (s, 2H), 7.39 (s, 1H), 7.47 (d, 1H, $J = 4.5$ Hz), 8.54 (d, 1H, $J = 3.2$ Hz). ^{13}C NMR (125 MHz, $CDCl_3$): δ 23.2, 121.0, 127.4, 127.6, 134.3, 135.0, 136.8, 142.8, 148.8, 155.5. HRMS calcd for $C_{12}H_9Cl_3N$ ($M^+ + H$) 238.0185, found 238.0190.

2.2. Synthesis of 9,9′-(5-(3-methylpyridin-2-yl)-1,3-phenylene) bis(9H-carbazole)

2-(3,5-Dichlorophenyl)-3-methylpyridine (2.0 g, 8.40 mmol), carbazole (3.51 g, 21.00 mmol), sodium *tert*-butoxide (4.04 g, 42.00 mmol), 2-dicyclohexylphosphino-2′,6′-dimethoxybiphenyl (0.86 g, 2.10 mmol), tris(dibenzylideneacetone)dipalladium (0.48 g, 0.52 mmol) and xylene (140 mL) were combined and heated under reflux under nitrogen for 36 h. The solution was cooled to room temperature and the organics were extracted into ethyl acetate, washed with distilled water, dried over magnesium sulfate, filtered. The solvent was removed in vacuo, and the product was isolated by column chromatography on silica gel (methylene chloride/*n*-hexane) to give 9,9′-(5-(3-methylpyridin-2-yl)-1,3-phenylene) bis(9*H*-carbazole) (1.95 g, 46% yield). Additional purification by sublimation (at 200 °C and 10^{-5} mm Hg) resulted in 1.5 g of pure compound (36% overall yield).

Light yellow powder, m.p. 132 °C, T_g 94 °C, FT-IR (KBr) 3047, 1590, 1450, 1334, 1311, 1229, 1155, 1120, 1026, 1002, 925, 806, 748, 710, 647 cm^{-1}. ^1H NMR (500 MHz, $CDCl_3$): δ 2.75 (s, 3H), 7.21 (t, 1H, $J = 4.2$ Hz), 7.30 (t, 4H, $J = 5.2$ Hz), 7.44 (t, 4H, $J = 5.3$ Hz), 7.58 (d, 4H, $J = 4.0$ Hz), 7.65 (s, 2H), 7.69 (d, 1H, $J = 4.8$ Hz), 7.85 (s, 1H), 8.13 (d, 4H, $J = 4.0$ Hz), 8.55 (d, 1H, $J = 3.3$ Hz). ^{13}C NMR (125 MHz, $CDCl_3$): δ 23.8, 109.5, 120.5, 121.3, 123.7, 124.1, 126.1, 126.2, 135.1, 137.1, 139.5, 140.5, 143.4, 148.9, 155.6. HRMS calcd for $C_{36}H_{25}N_3$ ($M^+ + H$) 500.2121, found 500.2127. Element analysis Calcd. for $C_{36}H_{25}N_3$ C(86.55%) H(5.04%) N(8.41%); found C(86.04%) H(5.08%) N(8.52%).

2.3. Device fabrication and measurements

Device structure of blue PHOLEDs was indium tin oxide (50 nm)/poly(3,4-ethylenedioxythiophene):poly(styrenesulfonate) (PEDOT:PSS, 60 nm)/4,4′-cyclohexylidenebis[*N,N*-bis(4-methyl phenyl)aniline] (TAPC, 20 nm)/1,3-bis(*N*-carbazolyl)benzene (mCP, 10 nm)/PPBC:iridium(III) bis[(4,6-difluorophenyl)-pyridinato-*N*,C^2] picolinate (FIrpic) (25 nm)/diphenylphosphine oxide-4-(triphenyl silyl)phenyl (TSPO1, 35 nm)/LiF(1 nm)/Al(200 nm). Doping concentrations of FIrpic were 3, 5, and 10%. PHWOLEDs had the device structure of ITO (50 nm)/PEDOT:PSS (60 nm)/TAPC (20 nm)/mCP (10 nm)/PPBC:FIrpic (15 nm)/1,3,5-tris(*N*-phenylbenzimidazole-2-yl)benzene (TPBI):iridium(III) bis(2-phenylquinoline) acetylacetonate($Ir(pq)_2acac$) (15 nm, 5%)/TSPO1 (35 nm)/LiF (1 nm)/Al (200 nm). The doping concentrations of FIrpic were 3, 5 and 10%. The doping concentration of FIrpic and $Ir(pq)_2acac$ was controlled by managing the evaporation rate of host and dopant materials. Hole only device with a device structure of ITO (50 nm)/PEDOT:PSS (60 nm)/TAPC (20 nm)/mCP (10 nm)/PPBC (25 nm)/TAPC (10 nm)/Al and electron only device with a device structure of ITO (50 nm)/Ca (5 nm)/PPBC (25 nm)/TSPO1 (35 nm)/LiF (1 nm)/Al (200 nm) were also prepared as single carrier devices. All devices were fabricated by vacuum thermal evaporation and were encapsulated with a glass lid after cathode deposition. The substrate and the glass lid were sealed using epoxy adhesive and CaO desiccant was inserted inside the device to capture moisture and oxygen. Current density–voltage characteristics of all devices were measured by Keithley 2400 source measurement unit and luminance performances were characterized by CS1000 spectroradiometer.

3. Results and discussion

The design of PPBC was based on carbazole and pyridine unit to obtain bipolar charge transport properties from the PPBC host material. The carbazole unit can play a role of a hole transport unit, while the pyridine unit can act as an electron transport unit, which can induce bipolar charge transport character in the PPBC host. In addition, a methyl substituent was attached to the pyridine unit to

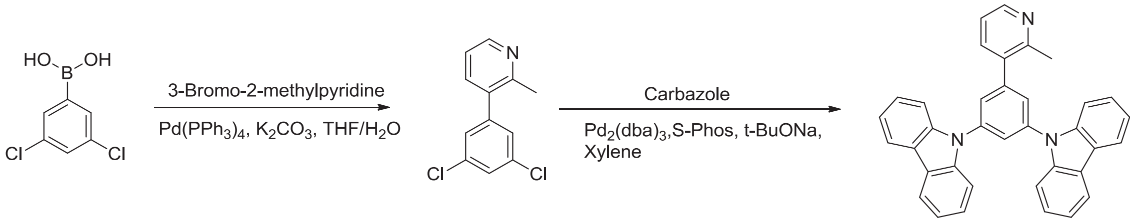

Scheme 1. Synthetic route of PPBC.

increase the triplet energy of the host material by reducing the conjugation length through steric hindrance.

The PPBC host was synthesized by Pd catalyst mediated coupling reaction between carbazole and 2-(3,5-dichlorophenyl)-3-methylpyridine which was prepared by Suzuki coupling reaction between (3,5-dichlorophenyl)boronic acid and 3-bromo-2-methylpyridine. Synthetic yield of the PPBC host was 36%. The PPBC host was purified by vacuum train sublimation after column chromatography and high purity level over 99% was obtained from high performance liquid chromatography. Chemical structure of the PPBC host was confirmed by NMR spectroscopy, elemental analysis and mass spectroscopy.

Photophysical properties of PPBC were analyzed using ultraviolet–visible (UV–Vis) absorption and photoluminescence (PL) spectrometers. Fig. 1 shows UV–Vis absorption, solution PL and low temperature PL spectra of the PPBC host. Strong UV–Vis absorption peaks were observed at 239 nm and 293 nm due to $\pi-\pi^*$ transition of the PPBC backbone and weak absorption peaks appeared at 324 nm and 338 nm because of $n-\pi^*$ transition of carbazole. UV–Vis absorption edge of PPBC was 345 nm, which corresponded to a bandgap of 3.59 eV. Maximum solution PL emission peak of PPBC was observed at 365 nm and solid PL emission was shifted to 388 nm due to intermolecular interaction of the PPBC host caused by electron donating carbazole and electron deficient pyridine. Phosphorescent emission of PPBC was measured in liquid nitrogen by applying delay time of 1 ms to exclude fluorescent emission. Peak position of the first phosphorescent emission was 414 nm, which corresponded to a triplet energy of 2.99 eV. The triplet energy of the PPBC host was higher than that of FIrpic (2.65 eV), indicating that the PPBC host can be suitable as the host material for blue PHOLEDs.

The highest occupied molecular orbital (HOMO) and the lowest unoccupied molecular orbital (LUMO) of PPBC were simulated using Gaussian 09 program. Fig. 2 shows the HOMO and LUMO of PPBC calculated using density functional of B3LYP with 6-31G* basis sets. The HOMO of PPBC was distributed over carbazole of PPBC because of electron donating character of carbazole, while the LUMO was dispersed over pyridine of PPBC due to electron deficiency of the pyridine unit. Therefore, the PPBC host can show bipolar charge transport properties.

The HOMO level of PPBC was −6.11 eV from the oxidation curve obtained by cyclic voltammetry measurement and the LUMO level was −2.52 eV from the HOMO and bandgap from UV–Vis absorption. The HOMO and LUMO levels of PPBC were suitable for hole injection from mCP (HOMO: −6.10 eV) and electron injection from TSPO1 (LUMO: −2.52 eV).

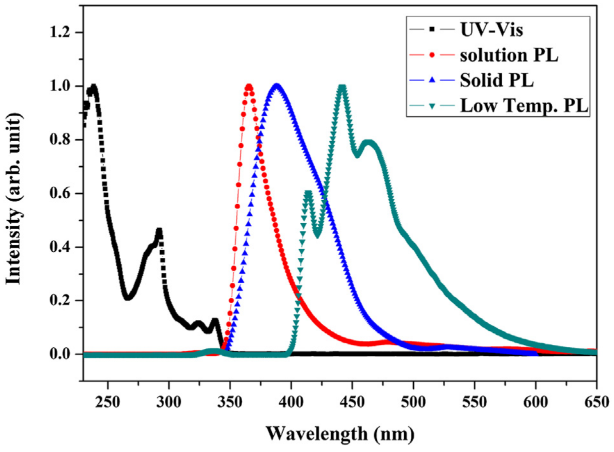

Fig. 1. UV–Vis, PL and low temperature PL spectra of PPBC.

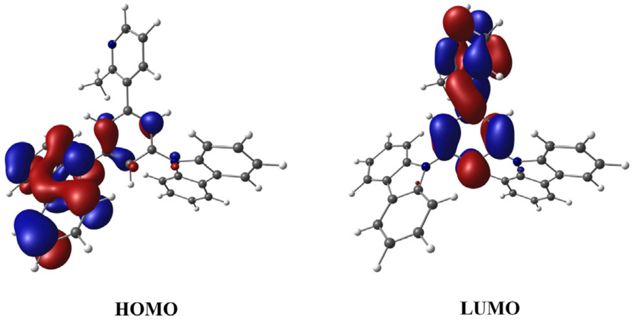

Fig. 2. HOMO and LUMO distribution of PPBC.

Hole only and electron only devices of PPBC were fabricated to compare hole and electron densities in the emitting layer. Current density–voltage curves of the single carrier devices are shown in Fig. 3. The current density of the electron only device was higher than that of hole only device, indicating that PPBC host material shows relatively strong electron transport properties. The electron deficient 3-methylpyridine unit improved electron transport properties of PPBC, resulting in relatively high electron density.

Blue PHOLEDs were fabricated using PPBC as the host material for FIrpic dopant. Fig. 4 shows current density–voltage–luminance curves of the blue PHOLEDs with the PPBC host according to the doping concentration of FIrpic. The current density and luminance of the PPBC devices were increased according to the doping concentration of FIrpic because of better electron injection at high doping concentration by electron trapping as reported in other works [16].

Quantum efficiency–current density curves of the PPBC devices are shown in Fig. 5. The quantum efficiency of the blue PHOLEDs was optimized at a doping concentration of 5% and a maximum quantum efficiency of 19.8% was obtained. The high quantum efficiency of the PPBC blue PHOLEDs can be explained by the efficient energy transfer and charge transport properties of PPBC. The triplet energy of the PPBC was higher than that of FIrpic and the PL emission of PPBC was overlapped with the UV–Vis absorption of FIrpic. Therefore, energy transfer from PPBC to FIrpic was efficient and contributed to the high quantum efficiency of the PPBC blue PHOLEDs. Charge balance in the emitting layer originated from the charge transport properties of PPBC also enhanced the quantum efficiency of the PPBC devices. As shown in the single carrier device data, relatively large electron current density was observed in the single carrier devices, which balanced holes and electrons in the

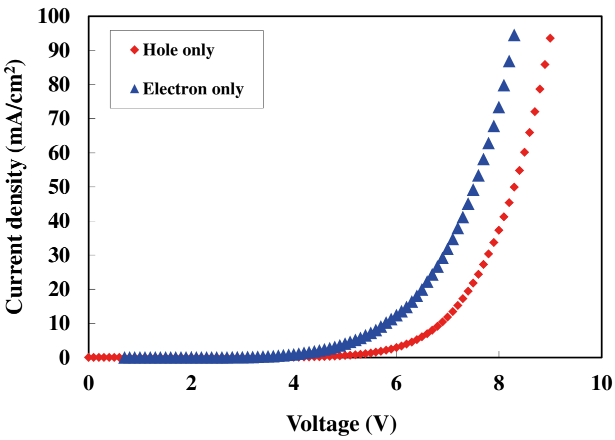

Fig. 3. Current density–voltage curves of hole only and electron only devices of PPBC.

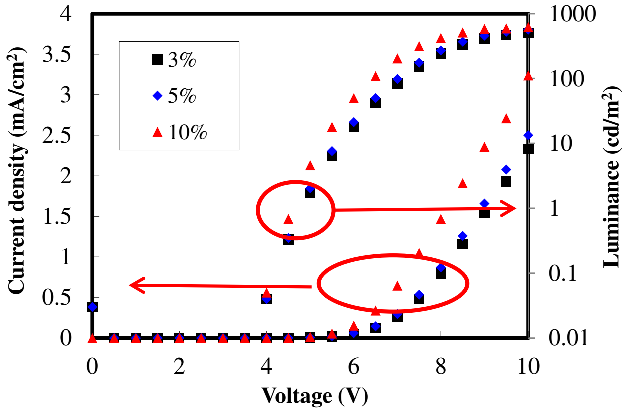

Fig. 4. Current density–voltage–luminance curves PPBC blue PHOLEDs according to the doping concentration of FIrpic.

emitting layer. The relatively high electron current density of the PPBC host is beneficial to balance holes and electrons in the emitting layer because the electron current density is reduced by electron trapping of the FIrpic dopant in the emitting layer.

Based on the high quantum efficiency of the PPBC blue devices, two color PHWOLEDs were developed by stacking an orange emitting layer on the PPBC blue emitting layer. The doping concentration of the blue emitting layer was managed to control the color of the PHWOLEDs because the FIrpic doping concentration can change the electron injection from the orange emitting layer to the blue emitting layer. The FIrpic doping concentrations were 5% and 10%. Current density–voltage–luminance curves of the PHWOLEDs are shown in Fig. 6. The current density and luminance of the PHWOLEDs was increased at high FIrpic doping concentration due to better electron injection into the blue emitting layer, which agrees with the current density dependence on the doping concentration of the PPBC blue devices.

Quantum efficiency–current density curves of the PHWOLEDs are presented in Fig. 7. The quantum efficiency of the PHWOLEDs was similar at 5% and 10% doping concentrations and a maximum quantum efficiency of 17.1% was obtained. The quantum efficiency at 1000 cd/m^2 was 14.9% and 15.3% at 5% and 10% doping concentrations, respectively. The high quantum efficiency of the PPBC blue PHOLEDs and bipolar charge transport properties of the PPBC host were effective to obtain high quantum efficiency through charge balance. Energy is transferred from the PPBC blue emitting layer to the orange emitting layer and the high efficiency of the PPBC blue emitting layer can boost the quantum efficiency of the PHWOLEDs.

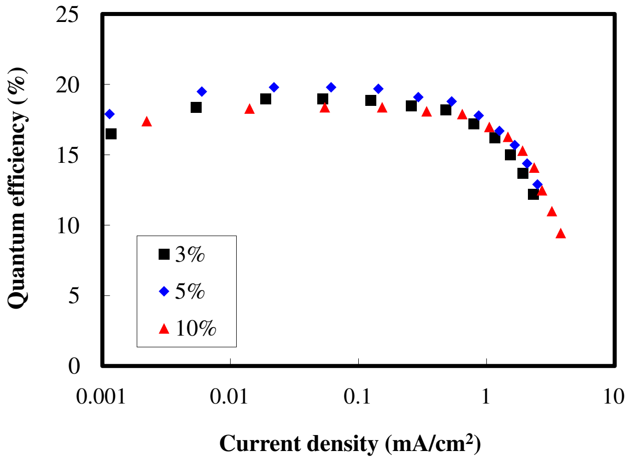

Fig. 5. Quantum efficiency–current density curves of PPBC blue PHOLEDs according to the doping concentration of FIrpic.

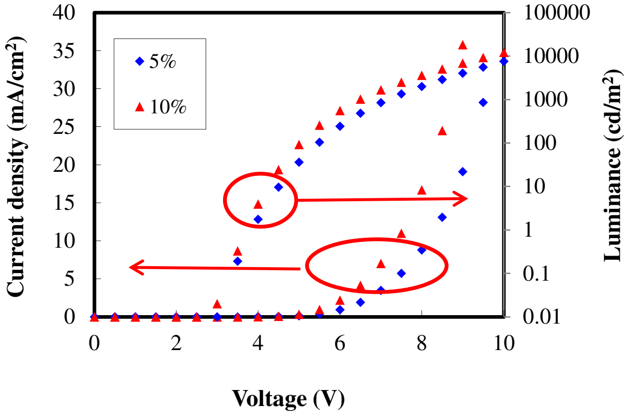

Fig. 6. Current density–voltage–luminance curves PPBC PHWOLEDs according to the doping concentration of FIrpic.

Electroluminescence spectra of the PHWOLEDs are shown in Fig. 8. The two devices exhibited two color white emission through blue emission from FIrpic and orange emission from Ir(pq)$_2$acac. The blue emission was intensified at high FIrpic doping concentration due to more electron injection from the orange emitting layer to the blue emitting layer. As explained in the blue PHOLEDs device data, electron density in the blue emitting layer is high at 10% doping concentration due to direct electron injection into the FIrpic dopant. Therefore, recombination zone of the PHWOLEDs is shifted from the orange emitting layer to the blue emitting layer, resulting in strong blue emission at 10% doping concentration. The color coordinates of the 5% and 10% FIrpic doped PHWOLEDs were (0.40, 0.33) and (0.34, 0.31) at 1000 cd/m^2, respectively.

Color stability of the PHWOLEDs was monitored from 100 cd/m^2 to 10,000 cd/m^2. Fig. 9 shows EL spectra of the PHWOLEDs doped with 10% FIrpic according to the luminance of the devices. There was little change of the EL spectra and the color coordinate was changed from (0.34, 0.31) at 100 cd/m^2 to (0.35, 0.31) at 10,000 cd/m^2. The good color stability of the PPBC PHWOLEDs is related with balanced charge injection between the blue and orange emitting layers. There is only 0.01 eV energy barrier for hole injection from the blue emitting layer to the orange emitting layer, which leads to

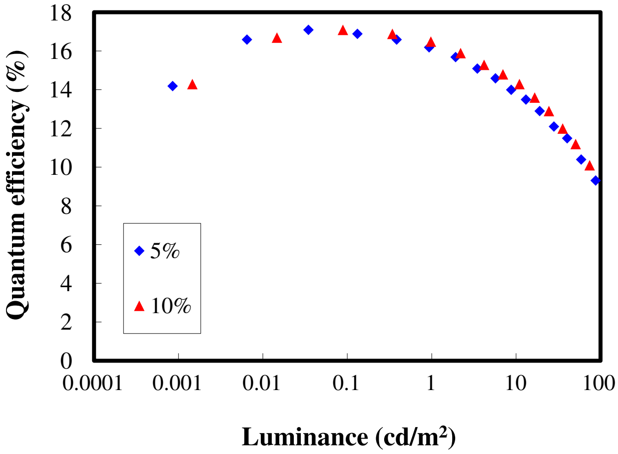

Fig. 7. Quantum efficiency–current density curves of the PPBC PHWOLEDs according to the doping concentration of FIrpic.

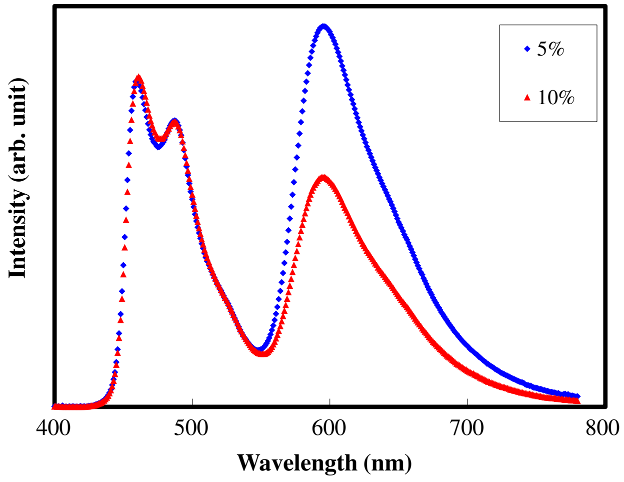

Fig. 8. Electroluminescence spectra of the PPBC PHWOLEDs according to the doping concentration of FIrpic.

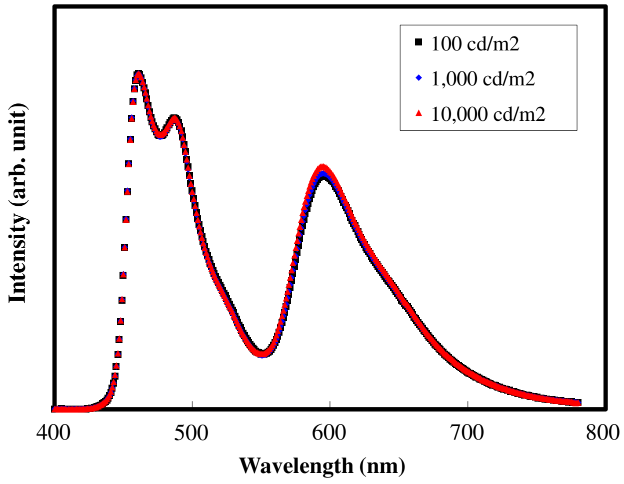

Fig. 9. Electroluminescence spectra of the PPBC PHWOLEDs doped with 10% FIrpic according to the luminance.

little field dependence of the hole injection on the driving voltage. The electron injection is also little affected by the electric field because the electron density is dominated by electron trapping of the FIrpic dopant. As there is no energy barrier for the direct electron injection from the TPBI emitting layer to the FIrpic dopant, the electron injection is also little influenced by the electric field. Therefore, the relative hole and electron density in the emitting layer is maintained constant and good color stability is observed. The use of the PPBC host was effective to obtain high quantum efficiency and good color stability.

4. Conclusions

In conclusion, high efficiency blue and white PHOLEDs were developed using PPBC bipolar host materials in the blue emitting layer. The PPBC host showed high triplet energy of 2.99 eV for efficient energy transfer to blue emitting FIrpic dopant and bipolar charge transport properties for hole and electron balance in the emitting layer. A high quantum efficiency of 19.8% in blue PHOLEDs and 17.1% in PHWOLEDs were achieved using the PPBC host material. In addition, the PPBC host was effective to obtain good color stability in the PHWOLEDs.

References

[1] Sun YR, Giebink NC, Kanno H, Ma B, Thompson ME, Forrest SR. Management of singlet and triplet excitons for efficient white organic light-emitting devices. Nature 2006;440:908–12.
[2] Schwartz G, Pfeiffer M, Reineke S, Walzer K, Leo K. Harvesting triplet excitons from fluorescent blue emitters in white organic light-emitting diodes. Adv Mater 2007;19:3672–6.
[3] Schwartz G, Reineke S, Rosenow TC, Walzer K, Leo K. Triplet harvesting in hybrid white organic light-emitting diodes. Adv Funct Mater 2009;19:1319–33.
[4] Anzenbacher Jr P, Montes VA, Takizawa SY. High-purity white light from a simple single dopant host-guest white organic light-emitting diode architecture. Appl Phys Lett 2008;93:163302–3.
[5] Ho CL, Wong WY, Wang Q, Ma D, Wang L, Lin Z. A multifunctional iridium-carbazolyl orange phosphor for high-performance two-element WOLED exploiting exciton-managed fluorescence/phosphorescence. Adv Funct Mater 2008;19:928–37.
[6] Wang Y, Hua Y, Wu X, Zhang L, Hou Q, Zhang N, et al. Application of mixed interface in white-electrophosphorescent devices: an efficient approach to adjust the distributions of carriers. Appl Phys Lett 2008;93:113302–3.
[7] Wang Y, Hua Y, Wu X, Zhang G, Hui J, Zhang L, et al. White electrophosphorescent devices based on tricolour emissive layers. J Phys D Appl Phys 2008;41:25104.
[8] Cheng G, Zhang Y, Zhao Y, Liu S, Ma Y. Improved efficiency for white organic light-emitting devices based on phosphor sensitized fluorescence. Appl Phys Lett 2006;88:83512–3.
[9] D'Andrade BW, Holmes RJ, Forrest SR. Efficient organic electrophosphorescent white-light-emitting device with a triple doped emissive layer. Adv Mater 2004;16:624–8.
[10] Cheng G, Zhang Y, Zhao Y, Lin Y, Ruan C, Liu S, et al. White organic light-emitting devices with a phosphorescent multiple emissive layer. Appl Phys Lett 2006;89:43504–13.
[11] Han C, Xie G, Xu H, Zhang Z, Xie L, Zhao Y, et al. A single phosphine oxide host for high-efficiency white organic light-emitting diodes with extremely low operating voltages and reduced efficiency roll-off. Adv Mater 2011;23:2491–6.
[12] Jeon SO, Yook KS, Joo CW, Lee JY. Phenylcarbazole-based phosphine oxide host materials for high efficiency in deep blue phosphorescent organic light-emitting diodes. Adv Funct Mater 2009;19:3644–9.
[13] Su S, Gonmori E, Sasabe H, Kido J. Highly efficient organic blue-and white-light-emitting devices having a carrier- and exciton-confining structure for reduced efficiency roll-off. Adv Mater 2008;20:4189–94.
[14] Williams EL, Haavisto K, Li J, Jabbour GE. Excimer-based white phosphorescent organic light-emitting diodes with nearly 100% internal quantum efficiency. Adv Mater 2007;19:197–202.
[15] Lee CW, Lee JY. High quantum efficiency in solution and vacuum processed blue phosphorescent organic light emitting diodes using a novel benzofuropyridine-based bipolar host material. Adv Mater 2013;25:596–600.
[16] Park HJ, Kim OY, Lee JY. Correlation of charge trapping and charge transport properties of blue triplet emitters with device performances of blue phosphorescent organic light-emitting diodes. Synth Met 2013;176:47–50.